Stagnation Point Flow and Heat Transfer of a Micropolar Fluid in a Porous Medium

Hazem A. ATTIA
Department of Mathematics, College of Science, Al-Qasseem University,
P.O. Box 237, Buraidah 81999, KSA

Abstract

The steady laminar flow in a porous medium of an incompressible non-Newtonian micropolar fluid impinging on a permeable flat plate with heat transfer is investigated. A numerical solution for the governing nonlinear momentum and energy equations is obtained. The effect of the porosity of the medium and the characteristics of the non-Newtonian fluid on both the flow and heat transfer is presented and discussed.

Key Words: Stagnation point flow, Porous medium, Fluid mechanics, Heat transfer, Finite difference.

1. Introduction

The two-dimensional flow of a fluid near a stagnation point is a classical problem in fluid mechanics. It was first examined by Hiemenz [1], who demonstrated that the Navier-Stokes equations governing the flow can be reduced to an ordinary third order differential equation using similarity transformation. Owing to the nonlinearities in the reduced differential equation, no analytical solution is available and the nonlinear equation is usually solved numerically, subject to two-point boundary conditions, one of which is prescribed at infinity.

Later, the problem of stagnation point flow was extended in numerous ways to include various physical effects. The axisymmetric three-dimensional stagnation point flow was studied by Homann [2]. The results of these studies are of great technical importance; for example, in the prediction of skin-friction, as well as heat/mass transfer near stagnation regions of bodies in high speed flows, and also in the design of thrust bearings and radial diffusers, drag reduction, transpiration cooling, and thermal oil recovery. In either the two- or three-dimensional case, Navier-Stokes equations governing the flow are reduced to an ordinary third order differential equation using a similarity transformation. The effect of suction on the Hiemenz problem has been considered in the literature. Schlichting and Bussman [3] were the first to give the numerical results. More detailed solutions were later presented by Preston [4]. An approximate solution to the problem of uniform suction is given by Ariel [5]. The effect of uniform suction on the Homann problem, where the flat plate is oscillating in its own plane, is considered by Weidman and Mahalingam [6]. In hydromagnetics, the problem of Hiemenz flow was chosen by Na [7] to illustrate the solution of a third-order boundary value problem using the technique of finite differences. An approximate solution of the same problem has been provided by Ariel [8]. Attia gave the effect of an externally applied uniform magnetic field on the two- [9] or three-dimensional [10] stagnation point flow in the presence of uniform suction or injection.

The study of heat transfer in boundary layer flows is of importance in many engineering applications, such as the design of thrust bearings and radial diffusers, transpiration cooling, drag reduction, and thermal recovery of oil. [11]. Massoudi and Ramezan [11] used a perturbation technique to solve for the stagnation point flow and heat transfer of a second grade non-Newtonian fluid. Their analysis is valid only for small values of the parameter that determines the behavior of the non-Newtonian fluid. Later, Massoudi and Ramezan [12] extended the problem to non-isothermal surfaces. Garg [13] improved the solution obtained by Massoudi [12] by numerically computing the flow characteristics for any value of the non-Newtonian parameter using a pseudo-similarity solution.

Non-Newtonian fluids have been considered by many researchers. Thus, among the non-Newtonian fluids, the solution of the stagnation point flow for viscoelastic fluids has been given by Rajeshwari and Rathna [14], Beard and Walters [15], Teipel [16], Arial [17], and others; for power-law fluids by Djukic [18] and for second grade fluids by Teipel [19]; by Ariel [20] in the hydrodynamic case and by Attia [21] in the hydromagnetic case. Stagnation point flow of a non-Newtonian micropolar fluid was studied by Nath [22] and Nazar et al. [23] in the hydrodynamic case.

The purpose of the present paper is to study the effect of the porosity of the medium on the steady laminar flow of an incompressible non-Newtonian micropolar fluid at a two-dimensional stagnation point with heat transfer. The wall and stream temperatures are assumed to be constant. The flow in the porous media deals with the analysis in which the differential equation governing the fluid motion is based on the Darcy's law, which accounts for the drag exerted by the porous medium [24-26]. A numerical solution is obtained for the governing momentum and energy equations using finite difference approximations, which take into account the asymptotic boundary conditions. The numerical solution computes the flow and heat characteristics for the entire range of the non-Newtonian fluid characteristics, the porosity parameter, and the Prandtl number.

2.   Formulation of the Problem

Consider the two-dimensional stagnation point flow of an incompressible non-Newtonian micropolar fluid impinging perpendicular on a permeable wall and flowing away along the x-axis, as shown in Fig. 1. This is an example of a plane potential flow, which arrives from the y-axis and impinges on a flat wall placed at $y=0$, divides into two streams on the wall, and leaves in both directions. The flow is through a porous medium, where the Darcy model is assumed [26]. The viscous flow must adhere to the wall, whereas the potential flow slides along it. (u,v) are the components for the potential flow of velocity at any point (x,y) for the viscous flow, whereas (U,V) are the velocity components for the potential flow. The velocity distribution in the frictionless flow in the neighborhood of the stagnation point is given by

$$U(x) = ax, V(y) = -ay$$

where the constant $a(>0)$ is proportional to the free stream velocity far away from the surface. The simplified two-dimensional equations governing the flow in the boundary layer of a steady, laminar, and incompressible micropolar fluid are [22,23]

$$\frac{\partial u}{\partial x} + \frac{\partial v}{\partial y} = 0, \tag{1}$$

$$\rho \left(u\frac{\partial u}{\partial x} + v\frac{\partial u}{\partial y} \right) = U\frac{dU}{dx} + (\mu + h)\left(\frac{\partial^2 u}{\partial y^2} \right) + h\frac{\partial N}{\partial y} + \frac{\mu}{K}(U(x) - u), \tag{2}$$

$$\rho \left(u\frac{\partial N}{\partial x} + v\frac{\partial N}{\partial y} \right) = \frac{\gamma}{j}\frac{\partial^2 N}{\partial y^2} - \frac{h}{j}\left(2N + \frac{\partial u}{\partial y} \right), \tag{3}$$
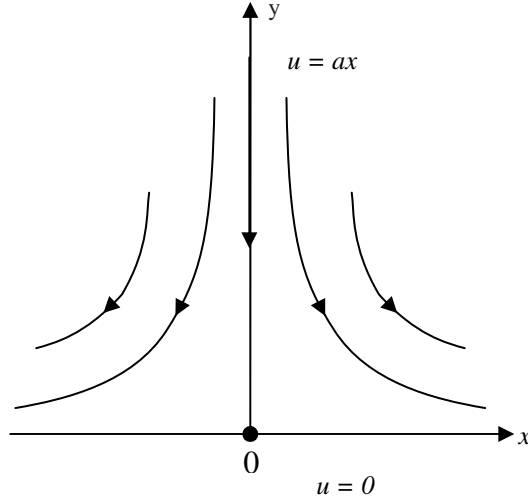
Figure 1. Physical model and coordinate system.

where N is the micro-rotation or angular velocity whose direction of rotation is in the x-y plane, μ is the viscosity of the fluid, ρ is the density of the fluid, $\bar{K}$ is the Darcy permeability [24-26], and j, γ, and h are the micro-inertia per unit mass, spin gradient viscosity, and vortex viscosity, respectively, which are assumed to be constant. The last term in the right-hand side represents the electromagnetic Lorentz force [24]. Here, γ is assumed to be given by [22,23]

$$\gamma = (\mu + h/2)j \tag{4}$$

and we take $j = \nu/a$ as a reference length and ν is the kinematic viscosity. Relation (4) is invoked to allow Eqs. (1)-(3) to predict the correct behaviour in the limiting case, when microstructure effects become negligible, and the microrotation, N, reduces to the angular velocity [23].

The appropriate physical boundary conditions of Eqs. (1)-(3) are

$$u(x,0) = 0, v(x,0) = 0, N(x,0) = -n\frac{\partial u}{\partial y}, \tag{5a}$$

$$y \to \infty : u(x,y) \to U(x) = ax, v(x,y) \to 0, N(x,y) \to 0, \tag{5b}$$

where n is a constant and $0 \le n \le 1$. The case $n = 1/2$ indicates the vanishing of the anti-symmetric part of the stress tensor and denotes weak concentration [23] of microelements, which will be considered here. The governing equations (1)-(4) subject to the boundary conditions (5) can be expressed in a simpler form by introducing the following transformation

$$\eta = \sqrt{\frac{a}{\nu}}y, u = axf'(\eta), v = -\sqrt{a\nu}f(\eta), N = ax\sqrt{\frac{a}{\nu}}g(\eta), g(\eta) = -\frac{1}{2}f''(\eta) \tag{6}$$

so that Eqs. (2) and (3) reduce to the single equation

$$\left(1 + \frac{K}{2}\right)f''' + ff'' - f'^2 + 1 + M(1 - f') = 0 \tag{7}$$

subject to the boundary conditions

$$f(0) = 0, f'(0) = 0, f'(\infty) = 1, \tag{8}$$

where $K = h/\mu(>0)$ is the material parameter, $M = \nu/a\bar{K}$ is the porosity parameter, and primes denote differentiation with respect to η. For micropolar boundary layer flow, the wall skin friction τ_w is given by

$$\tau_w = \left[(\mu + h)\frac{\partial u}{\partial y} + hN \right]_{y=0} \tag{9}$$

Using $U(x) = ax$ as a characteristic velocity, the skin friction coefficient C_f can be defined as

$$C_f = \frac{\tau_w}{\rho U^2}, \tag{10}$$

Substituting (6) and (9) into (10), we get

$$C_f Re_x^{1/2} = (1 + K/2)f''(0) \tag{11}$$

where $Re_x^{1/2} = xU/\nu$ is the local Reynolds number.

Using the boundary layer approximations and neglecting the dissipation, the equation of energy for temperature T is given by [11,12],

$$\rho c_p \left(u\frac{\partial T}{\partial x} + v\frac{\partial T}{\partial y} \right) = k\frac{\partial^2 T}{\partial y^2} \tag{12}$$

where c_p is the specific heat capacity at constant pressure of the fluid, and k is the thermal conductivity of the fluid. A similarity solution exists if the wall and stream temperatures, T_w and T_∞ are constants–a realistic approximation in typical stagnation point heat transfer problems [11,12].

The boundary conditions for the temperature field are

$$y = 0 : T = T_w, \tag{13a}$$

$$y \to \infty : T \to T_\infty, \tag{13b}$$

Introducing the non-dimensional variable

$$\theta = \frac{T - T_\infty}{T_w - T_\infty},$$

and using the similarity transformations given in Eq. (6), we find that Eqs. (12) and (13) reduce to,

$$\theta'' + \Pr f\theta' = 0 \tag{14}$$

$$\theta(0) = 1, \theta(\infty) = 0, \tag{15}$$

where $\text{Pr} = \mu c_p / k$ is the Prandtl number.

The heat transfer at the wall is computed from Fourier's law [11,12] as follows:

$$q_w = -k\left(\frac{\partial T}{\partial y}\right)_{y=0} = -k(T_\infty - T_w)\sqrt{\frac{a}{\nu}}G(\text{Pr})$$

where G is the dimensionless heat transfer rate that is given by

$$G^{-1} = \int\limits_0^\infty d\eta \exp(-2\,\text{Pr}\int\limits_0^\eta f\,ds).$$

The flow Eqs. (7) and (8) are decoupled from the energy Eqs. (14) and (15), and need to be solved before the latter can be solved. The flow Eq. (7) constitutes a non-linear, non-homogeneous boundary value problem (BVP). In the absence of an analytical solution of a problem, a numerical solution is, indeed, an obvious and natural choice. The boundary value problem given by Eqs. (7) and (8) may be viewed as a prototype for numerous other situations, which are similarly characterized by a boundary value problem having a third order differential equation with an asymptotic boundary condition at infinity. Therefore, its numerical solution merits attention from a practical point of view. The flow Eqs. (7) and (8) are solved numerically using finite difference approximations. A quasi-linearization technique is first applied to replace the non-linear terms at a linear stage, with the corrections incorporated in subsequent iterative steps until convergence. The quasi-linearized form of Eq. (7) is,

$$(1 + K/2)f'''_{n+1} + f_n f''_{n+1} + f''_n f_{n+1} - f''_n f_n - 2f'_n f'_{n+1} + f'^2_n + 1 + M(1 - f'_{n+1}) = 0$$

where the subscript n or $n + 1$ represents the nth or $(n + 1)^{th}$ approximation to the solution. Then, the Crank-Nicolson method is used to replace the different terms by their second order central difference approximations. An iterative scheme is used to solve the quasi-linearized system of difference equations. The solution for the Newtonian case is chosen as an initial guess and the iterations are continued until convergence within prescribed accuracy. Finally, the resulting block tri-diagonal system was solved using generalized Thomas' algorithm.

The energy Eq. (14) is a linear second order ordinary differential equation with a variable coefficient, f(η), which is known from the solution of flow Eqs. (7) and (8) and the Prandtl number Pr is assumed constant. Equation (14) is solved numerically under the boundary condition (15) using central differences for the derivatives and Thomas' algorithm for the solution of the set of discretized equations. The resulting system of equations has to be solved in the infinite domain $0 < \eta < \infty$. A finite domain in the η-direction can be used instead, with η chosen large enough to ensure that the solutions are not affected by imposing the asymptotic conditions at a finite distance. Grid-independence studies show that the computational domain $0 < \eta < \eta_\infty$ can be divided into intervals, each of uniform step size, which equals 0.02. This reduces the number of points between $0 < \eta < \eta_\infty$ without sacrificing accuracy. The value $\eta_\infty = 10$ was found to be adequate for all the ranges of parameters studied here. Convergence is assumed when the ratio of each f, f', f'', or f''' for the last two approximations differed from unity by less than 10^{-5} at all values of η in $0 < \eta < \eta_\infty$.

3.   Results and Discussion

Figures 2 and 3 present the velocity profiles of f and f', respectively, for various values of K and M. The figures show that increasing the parameter K decreases both f and f', while its effect is more pronounced

for higher M. Increasing M increases them and its effect is more apparent for higher K. Also, increasing K increases the velocity boundary layer thickness, while increasing M decreases it due to its resistive effect.
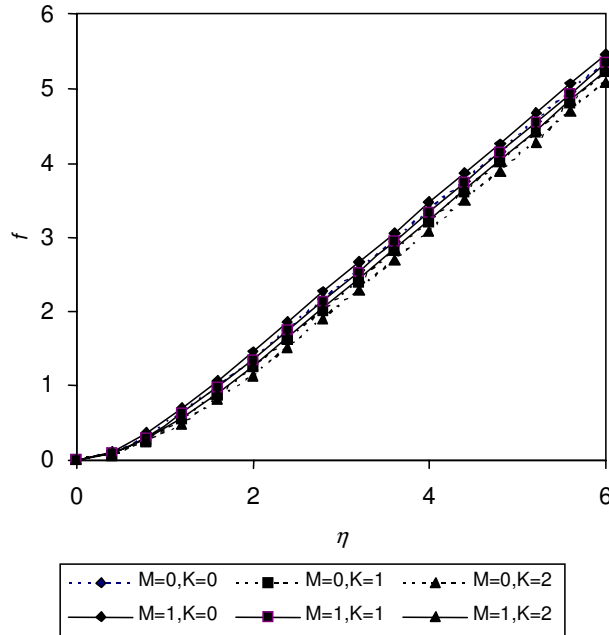

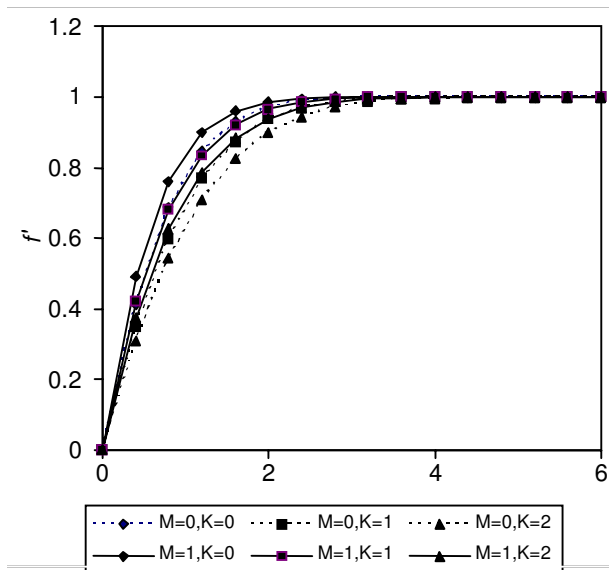**Figure 2.** Effect of the parameters K and M on the profile of f.

Figure 3. Effect of the parameters K and M on the profile of f'.

Figure 4 presents the profile of temperature θ for various values of K and M, and Pr $= 0.5$. It is clear that increasing K increases θ and the thickness of the thermal boundary layer. Increasing M decreases the thermal boundary layer thickness for all K. Figure 5 presents the temperature profile for various values of K and Pr, and for $M = 0.5$. This figure brings out clearly the effect of the Prandtl number on the thermal boundary layer thickness. As shown in Fig. 5, increasing Pr decreases the thermal boundary layer thickness for all K. It is clear that increasing K decreases θ and the effect of K on θ is more pronounced for higher values of Pr.
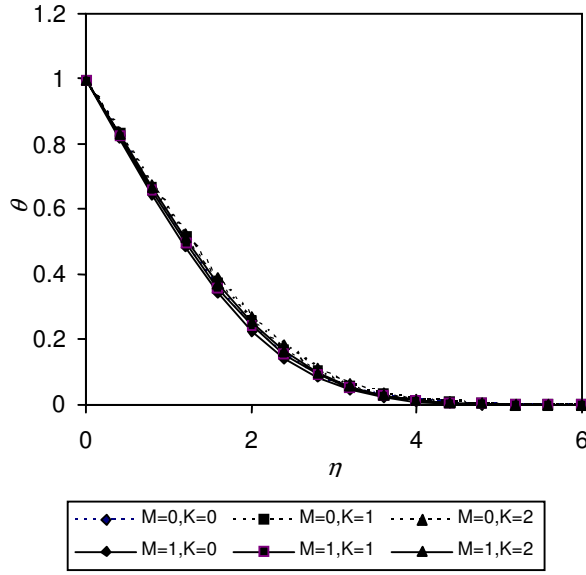
Figure 4. Effect of the parameters K and M on the profile of θ (Pr $= 0.5$).
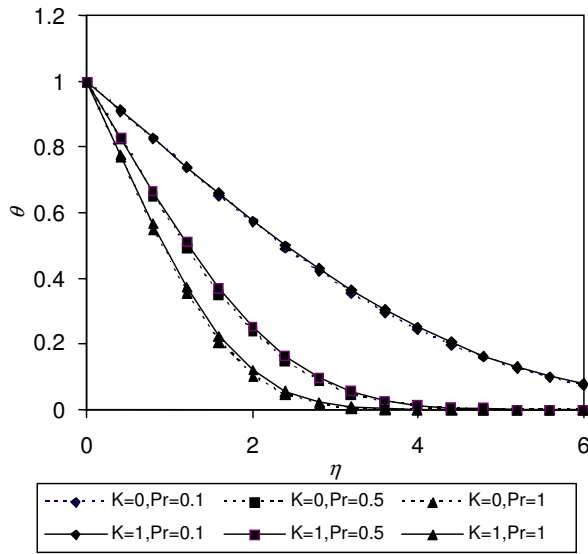

Figure 5. Effect of the parameters K and Pr on the profile of θ ($M = 0.5$).

Tables 1 and 2 present the variation of the wall shear stress $C_f Re_x^{1/2}$ and the heat transfer rate at the wall $G(\text{Pr})$, respectively, for various values of K and M, and for Pr $= 0.5$. Table 1 shows that for all M, increasing K increases $C_f Re_x^{1/2}$ and then, increasing K further decreases $C_f Re_x^{1/2}$. Increasing M increases $C_f Re_x^{1/2}$ steadily for all K and its effect is more apparent for smaller K. Table 2 shows that increasing K decreases $G(\text{Pr})$ while increasing M increases $G(\text{Pr})$ for all K.

Table 3 presents the effect of K on G(Pr) for various values of Pr and for $M = 0.5$. Increasing K decreases G(Pr) for all Pr and its effect is greater for higher Pr. Increasing Pr increases $G(\text{Pr})$ for all K. Table 4 shows the variation of $G(\text{Pr})$ for various values of Pr and M and, for $K = 0.5$. Increasing M increases $G(\text{Pr})$ and its effect is more apparent for higher Pr. Increasing Pr increases G steadily for all M and its effect is more apparent for higher M.

Table 1. Variation of the wall shear stress $C_f Re_x^{1/2}$ with K and M.

M	K = 0	K = 0.5	K = 1	K = 1.5	K = 2
0	1.2326	1.7915	1.7612	1.7469	1.7431
0.5	1.3294	1.9322	1.8995	1.8842	1.8800
1	1.5853	2.3041	2.2652	2.2469	2.2419
1.5	1.9389	2.8181	2.7705	2.7482	2.7421
2	2.3466	3.4107	3.3530	3.3260	3.3186

Table 2. Variation of the wall heat transfer $G(\mathrm{Pr})$ with K and M (Pr = 0.5).

M	K = 0	K = 0.5	K = 1	K = 1.5	K = 2
0	0.4352	0.4258	0.4178	0.4109	0.4050
0.5	0.4399	0.4307	0.4229	0.4162	0.4103
1	0.5411	0.4423	0.4349	0.4284	0.4228
1.5	0.4637	0.4555	0.4485	0.4405	0.4371
2	0.4754	0.4677	0.4612	0.4555	0.4504

Table 3. Variation of the wall heat transfer $G(\mathrm{Pr})$ with K and Pr (M = 0.5).

K	Pr = 0.05	Pr = 0.1	Pr = 0.5	Pr = 1	Pr = 1.5
0	0.1674	0.2219	0.4399	0.5812	0.6809
0.5	0.1659	0.2191	0.4307	0.5671	0.6632
1	0.1645	0.2166	0.4229	0.5553	0.6486
1.5	0.1633	0.2144	0.4162	0.5453	0.6363
2	0.1622	0.2124	0.4103	0.5367	0.6256

Table 4. Variation of the wall heat transfer $G(\mathrm{Pr})$ with M and Pr (K = 0.5).

M	Pr = 0.05	Pr = 0.1	Pr = 0.5	Pr = 1	Pr = 1.5
0	0.1648	0.2176	0.4258	0.5594	0.6535
0.5	0.1659	0.2191	0.4307	0.5671	0.6632
1	0.1677	0.2225	0.4423	0.5852	0.6864
1.5	0.1697	0.2263	0.4555	0.6061	0.7133
2	0.1715	0.2298	0.4677	0.6258	0.7387

4. Conclusions

The two-dimensional stagnation point flow of an incompressible non-Newtonian micropolar fluid with heat transfer through a porous medium was studied. A numerical solution for the governing equations is obtained, which allows the computation of the flow and heat transfer characteristics for various values of the non-Newtonian parameter K, the porosity parameter M, and the Prandtl number Pr. The results indicate that increasing the parameter K increases both the velocity and thermal boundary layer thickness, while increasing M decreases the thickness of both layers. The effect of the material parameter K on the velocity is more apparent for higher M. The influence of K or M on the temperature is more apparent for higher values of Prandtl number.

References

[1] K. Hiemenz, *Dingler Polytech* J., **326**, (1911), 321.

[2] F. Homann, *Z. Angew. Math. Mech.*, **16**, (1936), 153.

[3] H. Schlichting and K. Bussmann, *Schri. Dtsch. Akad. Luftfahrtforschung*, Ser. B, **7**, (1943), 25.

[4] J. Preston, Reports and memoirs, *British Aerospace Research Council, London*, No. 2244, (1946).

[5] P. Ariel, *J. Appl. Mech.*, **61**, (1994), 976.

[6] P. Weidman and S. Mahalingam, *J. Engg. Math.*, **31**, (1997), 305.

[7] T. Na, *Computational methods in engineering boundary value problem,* (Academic Press, New York,1979).

[8] P. Ariel, *Acta Mech.*, **103**, (1994), 31.

[9] H. Attia, *Arab. J. Sci. Engg.*, **28**(1B), (2003), 107.

[10] 10. H. Attia, *Can. J. Phys.*, **81**, (2003), 1223.

[11] M. Massoudi and M. Ramezan, *ASME HTD*, **130**, (1990), 81.

[12] M. Massoudi and M. Ramezan, *Mech. Res. Commun.*, **19**(2), (1992), 129.

[13] V. Garg, *Acta Mech.*, **104**, (1994), 159.

[14] G. Rajeshwari and S. Rathna, *Z. Angew. Math. Phys.*, **13**, (1962), 43.

[15] D. Beard and K. Walters, *Proc. Cambridge Philos. Soc.*, **14**, (1992), 757.

[16] I. Teipel, *Rheological Acta*, **25**, (1986), 75.

[17] P. Ariel, *International J. Numerical Methods Fluids*, **14**, (1992), 757.

[18] D. Djukic, *ASME J. Appl. Mech.*, **40**, (1974), 822.

[19] I. Teipel, *CSME Trans.*, **12**(2), (1988), 57.

[20] P. Ariel, *J. Comput. Appl. Math.*, **59**(1), (1995), 9.

[21] H. Attia, *Can. J. Phys.*, **78**, (2000), 875.

[22] G. Nath, *Rheological Acta*, **14**, (1975), 850.

[23] R. Nazar, N. Amin, D. Filip, and I. Pop, *International J. of Non-Linear Mechanics*, **39**, (2004), 1227.

[24] D. Joseph, D. Nield, G. Papanicolaou, *Water Resources Research*, **18**(4), (1982), 1049.

[25] D. Ingham and I. Pop, *Transport phenomena in porous media*, (Pergamon, Oxford, 2002).

[26] A. Khaled and K. Vafai, *Int. J. Heat Mass Transfer*, **46**, (2003), 4989.